

Carbon Nanofiber Nanoelectrode Array: Effect of Process Conditions on Reliability

Uchechukwu C. Wejinya, *Member, IEEE*, Siva Naga Sandeep Chalamalasetty, *Student Member, IEEE*, Zhuxin Dong, *Student Member, IEEE*, Prabhu U. Arumugam, and Meyya Meyyappan, *Fellow, IEEE*

Abstract—Nanoelectrode arrays (NEA) using 1-D nanomaterials as the electrode material have shown promise for biosensing applications. Vertical, freestanding, individual carbon nanofibers (CNFs) on patterned substrates constitute one example of NEA in the literature. The development of a biosensor system using this NEA first requires reliability studies prior to undertaking system integration with microfluidics and sample handling aspects. Here, we have investigated the effect of temperature and process conditions on the diameters and quality of the CNFs using atomic force microscopy (AFM). A Taguchi approach is employed to study the temperature effect in etched and unetched CNFs using AFM followed by a statistical analysis.

Index Terms—Carbon nanofiber (CNF), process conditions, reliability, statistical analysis.

I. INTRODUCTION

IN the last ten years since the introduction of the U.S. National Nanotechnology Initiative, nanomaterials have been extensively explored for electronics, optoelectronics, chemical sensors, biosensors, and other applications. While the science has advanced rapidly as evidenced by the growth in the nanoscience and technology literature, there is no commercial product in the market in any of the aforementioned areas. The reasons include issues and problems related to the reproducible growth or preparation of nanomaterials with desirable properties, development of large scale manufacturing techniques suitable for dealing with nanomaterials and nanoscale features, and focus on engineering issues associated with product development beyond the basic science. The development of nanobiosensors for lab-on-a-chip, environmental monitoring, pathogen detection, cancer

diagnostics, and other applications is one example facing commercialization challenge despite the enormous work on the use of nanoparticles quantum dots, nanowires (of silicon, ZnO, etc.) and carbon nanotubes (CNTs) for biosensing [1]–[16]. In this study, we focus on carbon nanofiber (CNF)-based nanoelectrode array (NEA) for biosensing applications and specifically address some reliability issues. The NEA consists of vertically aligned CNFs (VACNFs) which are individual and freestanding, 50–70 nm in diameter and positioned precisely on prespecified locations using patterning techniques [6], [7]. Individual electrodes are isolated from each other with a dielectric insulation (SiO_2) and therefore only tips of the VACNFs are exposed. The tips are functionalized with a specific probe (DNA, antibody, aptamer, etc.) chosen for binding with a target of interest. In practice, the unfunctionalized NEA can be shipped to a customer wherein it can be functionalized with the probe for further immediate use. In another scenario, functionalized NEAs can be stored for later use. In any such practical situation, the effects of temperature, humidity, and chemical processes on the diameter and exposed length of VACNFs are important to understand for the reliable use of the biosensors in the field. Here, we use atomic force microscopy (AFM) to study the effects of temperature and chemical etchants on the dimensions of VACNF. The Taguchi approach [17] is used to design the experiments, and the results are analyzed statistically. A regression line equation is developed for the experimental data and then compared with available theory [18] relating nanostructure dimensions to temperature.

II. FABRICATION OF NANO-ELECTRODE ARRAY CHIPS

Our approach to fabricate the VACNF-NEAs has been described previously [6], [7] and some relevant details are given below in the context of the reliability study to be performed here. The fabrication includes six major steps done on a 4-in silicon (1 0 0) wafer coated with 500 nm of silicon dioxide. The fabrication process is shown in Fig. 1 and the steps include (a) metal deposition; (b) nanopatterning of Ni catalyst dots; (c) directional growth of CNFs; (d) silicon dioxide deposition for electrical isolation and mechanical support; (e) chemical mechanical polishing (CMP) to expose CNF tips, and (f) a wet etch with 7:1 HF to expose the electrical contact pads.

A. Deposition of Metal

In this step, metal is deposited for micropads, contact pads, and interconnects. A single 4-in Si wafer is lithographically patterned for nine micropads, nine contact pads, and channels

Manuscript received March 15, 2011; revised November 30, 2011 and June 6, 2012; accepted October 9, 2012. Date of publication December 11, 2012; date of current version January 4, 2013. This work was supported in part by the University of Arkansas, College of Engineering External Mentoring Award Program. The review of this paper was arranged by Associate Editor L. Dong.

U. C. Wejinya and Z. Dong are with the Department of Mechanical Engineering, University of Arkansas, Fayetteville, AR 72701 USA (e-mail: uwejinya@uark.edu; dzhuxin@uark.edu).

S. N. S. Chalamalasetty is with the Department of Microelectronics and Photonics, University of Arkansas, Fayetteville, AR 72701 USA (e-mail: schalama@uark.edu).

P. U. Arumugam was with the Center for Nanotechnology, NASA Ames Research Center, Moffett Field, CA 94035 USA. He is now with the Advanced Diamond Technologies, Romeoville, IL 60446 USA (e-mail: auprabhu@yahoo.com).

M. Meyyappan is with the NASA Ames Research Center, Moffett Field, CA 94035 USA (e-mail: m.meyyappan@nasa.gov).

Color versions of one or more of the figures in this paper are available online at <http://ieeexplore.ieee.org>.

Digital Object Identifier 10.1109/TNANO.2012.2227496

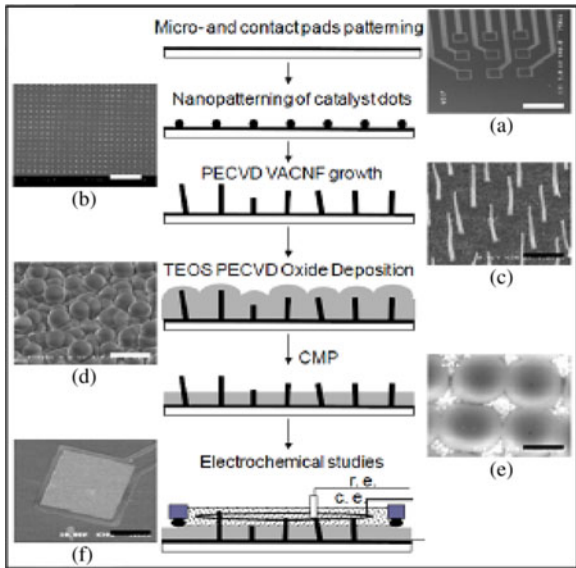


Fig. 1. Fabrication steps and the changes on the wafer can be seen in the pictures inset. (a) Deposition of metal, (b) nanopatterning, (c) growth of CNFs, (d) deposition of silicon dioxide, and (e) CMP.

for interconnects. Electron beam evaporation is used to deposit a 200-nm thick Cr film and then the wafer is immersed in acetone for 1 h. Once removed from acetone, the wafer is sprayed with methanol and isopropyl alcohol (IPA) and blown dry with N_2 .

B. Nanopatterning of Ni Catalyst Dots

Using e-beam lithography, Ni dots are patterned onto the substrate. Approximately 39 000 Ni catalyst dots are patterned onto each of the micropads. A 400-nm thick Poly(methylmethacrylate) (PMMA) A7 is spun coated at 3000 r/min , baked at 180 $^{\circ}C$ for 90 s, and exposed at 100 K-eV, 2 nA, 1950 $\mu C/cm^2$. Exposures are developed in a solution of 1:1 methyl isobutyl ketone (MIBK):IPA for 2 min, immersed in IPA for 30 s, and blown dry with N_2 . Subsequently, the patterned catalyst dots are verified using an optical microscope and a 10-nm Cr followed by 30-nm Ni catalyst is deposited by electron beam evaporation at $\sim 2 \text{ \AA}/s$. The coated wafers are immersed in acetone for 1 h. The wafers are then removed from the acetone while being sprayed with IPA and then blown dry with N_2 .

C. Directional Growth of VACNFs

The next step is directional growth of VACNFs on the nickel dots created in step B. A dc-biased plasma-enhanced chemical vapor deposition (PECVD) is employed at a processing pressure of 6.3 mbar, plasma power of 180 W and 700 $^{\circ}C$, 125 sccm C_2H_2 feedstock, and 444 sccm NH_3 diluent. Then, a 5-min thermal annealing at 600 $^{\circ}C$ is carried out before initiating the plasma with 250 sccm NH_3 . To attain the required growth temperatures and thermal anneal, a 60 $^{\circ}C/min$ thermal gradient is used. A 15 min growth run produces CNFs of height 1.5 μm , base diameter 100 nm, and tip diameter 70 nm on average. At this step scanning electron microscopy is used to validate the results.

D. Deposition of Silicon Dioxide

In order to passivate the sidewalls of nanofibers, a $3 \mu m \pm 0.8\%$ of SiO_2 layers are deposited onto the wafers using a pressure of 3 Torr, temperature of 400 $^{\circ}C$, and RF power of 1000 W. A mixture of ~ 6000 sccm of O_2 and 2–3 mL/min of Tetraethyl orthosilicate is used in a parallel plate dual RF PECVD to obtain highly conformal coating of SiO_2 on newly created nanofibers and interconnects.

E. Chemical Mechanical Polishing

Surface polarization along with exposing the nanofiber tips is attained by removal of excess SiO_2 and partial removal of nanofiber tip using CMP. This process involves removing the existing material with 0.5- μm alumina (pH 4) at 10 mL/min, 60-r/min platen, 15-r/min carrier, and 15 psig down force at 150 nm/min for polishing.

F. Wet Etch

This is the final step in the fabrication of VACNFs. In general, wet etch is used for the exposure of contact pads which are covered with SiO_2 . A 7:1 diluted HF solution is used to etch oxide at a rate of $\sim 15 \text{ \AA}/s$. Wafers are then diced for individual chips.

III. EXPERIMENTAL SETUP

The fabricated unetched and hydrogen fluoride (HF)-etched nanofiber chips are now subjected to variable temperatures at constant humidity and changes in the dimensions of the nanofiber are recorded. A Microclimate Environmental Chamber (manufactured by Cincinnati Sub-Zero (CSZ): model No. MCBH 1.3) is used for this study. With an error of $\pm 0.5\%$ in the range of $-20 \text{ }^{\circ}C$ –100 $^{\circ}C$, the temperature measurement is precise and accurate. In this method, the environmental chamber is set to a fixed temperature and relative humidity. After attainment of the set parameters, the chip with fabricated nanofibers is placed in the environmental chamber for 30 min at the set temperature allowing the nanofibers to respond to that particular temperature and then cooled back to the room temperature of 23 $^{\circ}C$ (the temperature inside the chamber when the chamber is not in operation). The chips are then treated in the dry box for less than 90 s to bring down the humidity to less than 3%, and then the dimensions are measured using the AFM (Agilent 5500-ILM) shown in Fig. 2. The scanning and characterization are done under acoustic ac imaging mode as shown in Fig. 3. The AFM probe utilized during imaging has a resonant frequency of 190 kHz and a spring constant of 48 N/m. During intermittent contact, the tip is brought close to the sample so that it lightly contacts the surface at the bottom of its travel, causing the oscillation amplitude to drop. Hence, we may completely ignore the influence of the cantilever tip during the dimension measurement as it cannot change anything of the target shape without contacting.

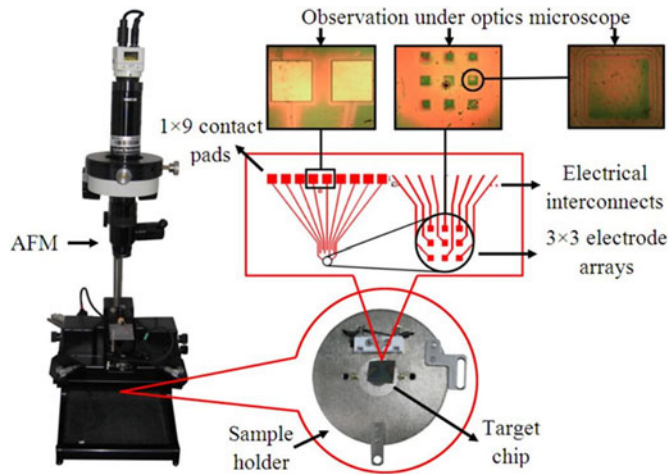


Fig. 2. AFM-based experimental setup showing the sample holder and chips for scanning and characterization.

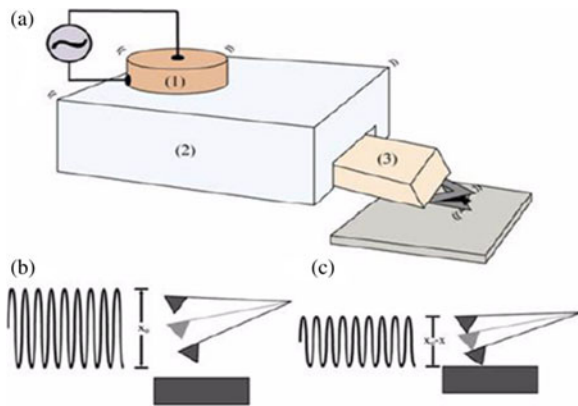


Fig. 3. AFM probe motion under acoustic AC Mode: (a) (1) ac applied to the nose cone; (2) base body of the cantilever beam; (3) cantilever beam with its tip; (b) and (c) cantilever driven to oscillate in sinusoidal motion.

IV. EXPERIMENTAL RESULTS

A. Environmental Chamber Treatment

Both the unetched and etched CNF chips are treated in the CSZ Microclimate environmental chamber at a fixed relative humidity of 10% and varying the temperature in the range of 0 °C–100 °C with 5 °C increment. The chips are treated for 30 min and then dried in dry box until the relative humidity falls below 3%. Even though the environmental chamber is operable in the range from –73 °C to 190 °C, due to the problem encountered in controlling the relative humidity at temperatures <10 °C, this experiment is conducted in the water temperature zone. The CNFs dimensions are then measured using AFM.

B. Scanning and Measurement

After the CNF chip is loaded into the scanner, one of the nine arrays is selected and the tip is lowered down to make it as close to the surface as possible, as shown in Fig. 4. The tip is never in contact with the surface and only touches the surface at regular intervals of time. In order to facilitate easy measurement of the nanofibers, a large area of $5\ \mu\text{m} \times 5\ \mu\text{m}$ is scanned first to locate

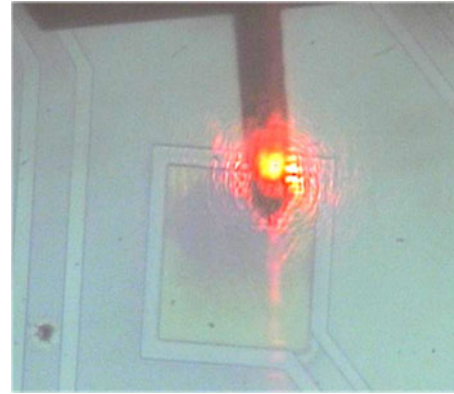


Fig. 4. AFM tip lowered onto the surface of the A2 array for measurement of nanofibers and topography study.

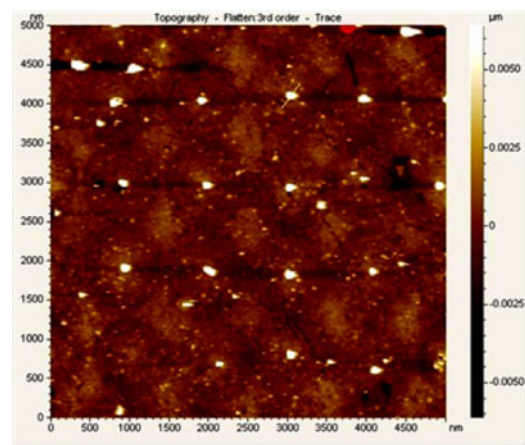


Fig. 5. 2-D cross sectional image of HF-etched substrate showing patterned CNFs. Cross-sectional area is $5\ \mu\text{m} \times 5\ \mu\text{m}$.

the nanofibers on the chip. After locating the CNFs, the scan area is reduced by zooming into a smaller area of $2\ \mu\text{m} \times 2\ \mu\text{m}$ so that a clear and distinct image of the nanofibers is found. Thus, after zooming in, CNFs are located once again this time with a better resolution, clear and distinct. Then, a line is drawn over the 2-D-generated image to obtain the topography graph.

A $25\text{-}\mu\text{m}^2$ 2-D cross-sectional image is shown in Fig. 5 where the patterned CNFs are clearly visible. Using e-beam lithography, Ni layer was patterned such that the distance between every two Ni dots is $1\ \mu\text{m}$.

Furthermore, the Agilent AFM used in the current experiment has a precision of 0.1 nm, so the VACNFs grown on patterned Ni dots can be clearly visualized. With this clear view of the CNFs, an area of approximately $2\ \mu\text{m}^2$ is zoomed in to get a better view of the fibers as shown in Fig. 6. By drawing a linear line across the fiber, a graphical 2-D image of the CNF is obtained from where we can measure the fiber dimensions.

The cross-sectional line drawn for the measurement of the nanofibers is shown in Fig. 7. Note that there is an increase in the cavities formed on the HF-etched substrate which shows the effect of the etchant on the substrate surface. From the generated topography image, nanofiber dimensions are calculated. The

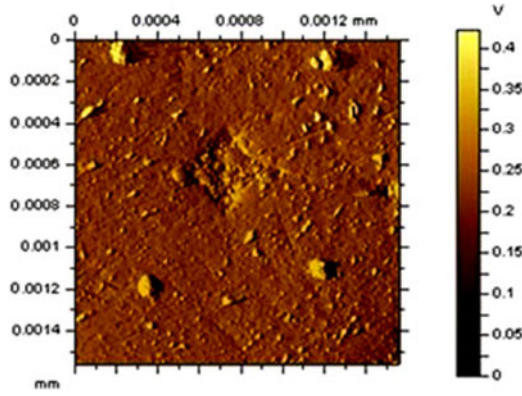


Fig. 6. 2-D cross-sectional image of HF-etched substrate from the AFM showing the patterned CNFs. Cross-sectional area is $1.2 \mu\text{m} \times 1.4 \mu\text{m}$.

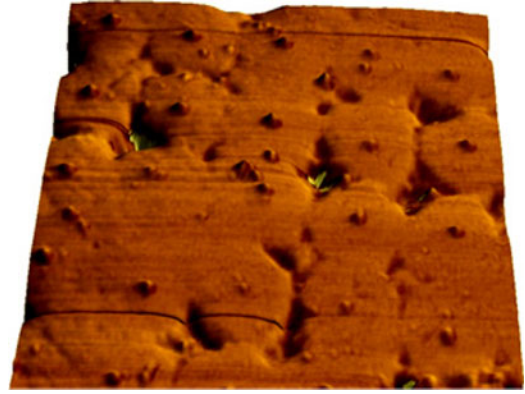


Fig. 9. 3-D topography image of unetched substrate at 20 °C. Patterned CNFs are clearly visible along with the cavities. Cross-sectional area is $5 \mu\text{m} \times 5 \mu\text{m}$.

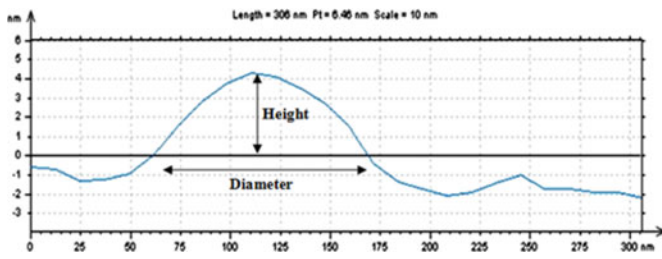


Fig. 7. Cross-sectional information for measurement based on line crossing (etched).

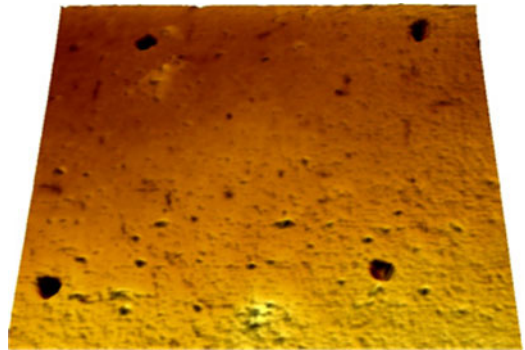


Fig. 10. 3-D topography image of etched substrate ($2 \mu\text{m} \times 2 \mu\text{m}$) with cavities in patterned areas.

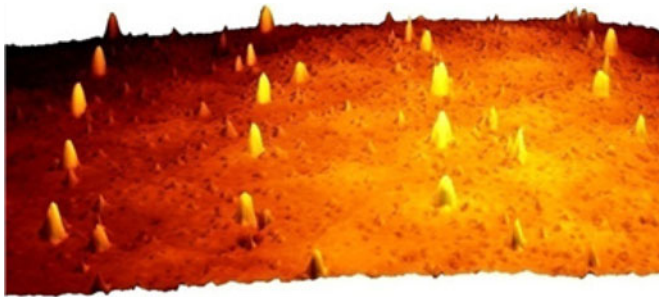


Fig. 8. 3-D topography of HF-etched substrate generated from 2-D cross section of $5 \mu\text{m} \times 5 \mu\text{m}$. Distance between any two peaks is $1 \mu\text{m}$.

horizontal distance of the curve where it intersects zero is the diameter of the carbon nanofiber while the vertical distance, i.e., from the baseline to the maximum point of the curve is the height of the CNF.

Fig. 8 shows the 3-D topography image of HF-etched substrate generated using the Picoimage software from Agilent Technologies. It is evident that there are free standing CNFs on the substrate surface and the distance between any two fibers is $1 \mu\text{m}$, which is expected because the nickel catalyst dots were patterned with the same $1\text{-}\mu\text{m}$ spacing. This image ensures that the measured dimensions are of nanofibers as they are perpendicular to the surface. To ensure the collected data accuracy, each array is measured at three different places and 10-D readings are recorded for each array. Thus, a total of 90 measurements are conducted for each temperature the substrate is subjected to.

Fig. 9 is the 3-D topography image of the unetched substrate generated using Picoimage software after exposure of the sub-

strate to 20 °C temperature for half hour. The cross-sectional area of the scan is $5 \mu\text{m} \times 5 \mu\text{m}$. Patterned CNFs are clearly visible with a separation distance between any two nanofibers of $1 \mu\text{m}$ affirming that they are CNFs. Cavities are observed along with the CNFs after the CMP process. Fig. 10 shows a 3-D topography image generated from the etched substrate surface. The cavities are observed in some regions which are more in a patterned manner and thus it can be inferred that the nanofiber probably got etched away indicating the etchant effect on the nanofiber. Thus, the electrodes on such locations will be ineffective.

C. Results and Discussion

As mentioned earlier, ten measurements are recorded per each NEA and on the whole 90 measurements are recorded for each temperature. This accumulates a large set of data for 20 different temperatures (from 0 °C to 100 °C with 5 °C increment).

Thus, the average-dimensional measurements are calculated for both unetched and HF-etched nanoelectrode chips and are tabulated along with their standard deviations in Tables I and II. Note that all the dimensional measurements are in nanometer and temperature is recorded in centigrade scale.

Figs. 11 and 12 are the graphical plots generated from the average-dimensional values versus temperature shown in Tables I and II. Fig. 11 shows the average height of unetched

TABLE I
NANOFIBER DIMENSIONS: AVERAGE AND STANDARD DEVIATION DATA FOR UNETCHED SUBSTRATE AT DIFFERENT TEMPERATURES

Temperature (°C)	RH	Avg. Diameter (nm)	Diameter Std. dev	Avg. height (nm)	Height Std. dev.
0	51.8	152.8	22.8	8.39	2.23
5	41.5	156.63	24.11	8.94	2.36
10	24.5	141.3	6.38	9.38	1.91
15	21.3	151.5	15.2	9.54	4.53
20	17	154.22	16.06	10.1	2.57
25	10	148.15	12.5	7.9	1.52
30	10	128.62	7.74	7.16	1.61
35	10	151.26	9.95	7.39	1.39
40	10	161.49	9.11	5.52	1.06
45	10	158.08	16.46	8.71	1.51
50	10	171.65	17.47	6.94	1.48
55	10	140.05	14.73	5.74	1.16
60	10	164.55	14.79	4.67	1.34
65	10	142.87	12.59	6	1.49
70	10	156.03	18.93	8.84	1.94
75	10	157.39	27.3	8.45	2.33
80	10	171.15	34.84	7.6	1.62
85	10	164.12	27.4	8.25	1.81
90	10	173.14	36.5	8.73	2.75
95	10	169.26	29.08	8.43	2.73
100	10	181.67	14.12	7.47	1.83

TABLE II
NANOFIBER DIMENSIONS: AVERAGE AND STANDARD DEVIATION DATA FOR HF-ETCHED SUBSTRATE AT DIFFERENT TEMPERATURES

Temperature (°C)	RH	Avg. Diameter (nm)	Diameter Std. dev	Avg. Height (nm)	Height Std. dev.
0	51.8	144.58	11.72	8.15	2.61
5	41.5	144.47	9.78	8.7	2.44
10	24.5	139.68	7.11	7.82	2.19
15	21.3	141.19	7.79	8.51	1.77
20	17	147.29	9.11	8.65	1.78
25	10	137.48	28.47	9.81	3.57
30	10	127.51	34.5	10.87	4.38
35	10	124.31	31.12	9.98	3.62
40	10	134.22	47.32	8.74	3.7
45	10	186.16	30.9	6.68	2.31
50	10	123.27	30.99	8.85	4.64
55	10	134.74	42.53	7.94	3.85
60	10	105.45	29.7	7.05	3.8
65	10	132.82	31.53	7.94	3.08
70	10	120.32	29.7	9.57	3.37
75	10	126.42	29.89	8.45	3.78
80	10	163.21	51.4	6.91	2.93
85	10	201.79	45.67	3.43	1.81
90	10	124.77	43.13	5.06	1.76
95	10	154.51	10.07	7.52	2.96
100	10	158.37	13.65	8	2.9

and HF-etched CNF sample versus temperature and then regression line equations are generated from the graphical data. Fig. 12 presents average diameter of unetched and HF etched versus temperature and then regression lines which fit the set of data are generated and their equations are shown in the image. From the regression line equations, it can be inferred that for both unetched and etched substrates, the diameter of the CNF increases with temperature, i.e., the change in diameter is directly proportional to the temperature and the positive slope of the regression line supports the claim. In contrast, the height of the CNFs for both unetched and etched decreases with the increase in temperature, i.e., change in height is inversely proportional to the temperature. The change in dimensions observed here is believed to be due to water vapor, and the conditions in the environmental chamber mimic the application environment to some extent. A reduction in the water vapor from the surface may result in increased exposure of the CNF and an increase in height.

The aforementioned observations are compared with theoretical results from Guisbiers and Buchailot next [18]. The equation in [18] given below is based on their work on superconductive, melting, Debye and Curie temperatures but not in

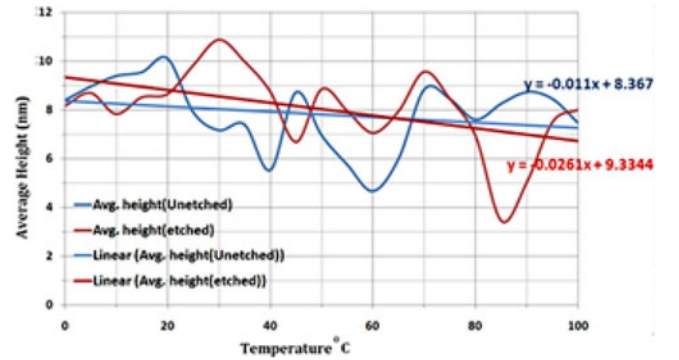


Fig. 11. Average height and temperature for both unetched and HF-etched samples along with their regression line equations.

normal ambient temperature range

$$\frac{T_x}{T_{x,\infty}} = \left(1 - \frac{\alpha}{D}\right)^{S - \frac{1}{2}} \quad (1)$$

where T_x is the surface temperature, $T_{x,\infty}$ is the bulk temperature, α is the height, D is the diameter, and S is the spin number.

This study on ambient temperature behavior of CNFs gives the following regression line equations for unetched average diameter [see (2)], etched average diameter [see (3)], unetched

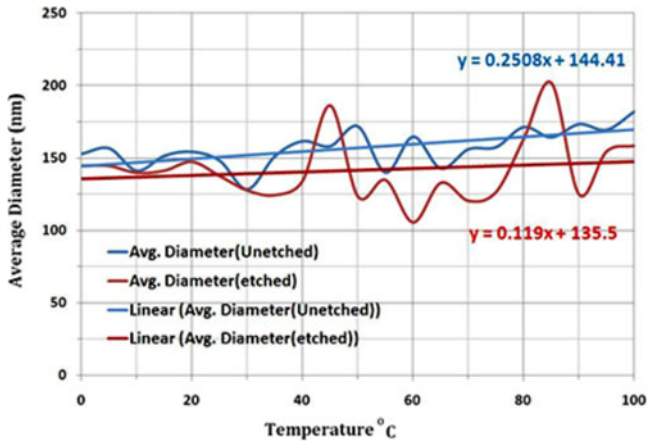


Fig. 12. Average diameter and temperature for both unetched and HF-etched samples along with their regression line equations.

average height [see (4)], and etched average diameter [see (5)]

$$\text{Dia}_{\text{unetched}} = 0.251x + 144.1 \quad (2)$$

$$\text{Dia}_{\text{etched}} = 0.12x + 135.5 \quad (3)$$

$$\text{Ht}_{\text{unetched}} = -0.01x + 8.34 \quad (4)$$

$$\text{Ht}_{\text{etched}} = -0.03x + 9.33 \quad (5)$$

where $\text{Dia}_{\text{unetched}}$ is the average diameter of unetched CNF in nanometer, $\text{Dia}_{\text{etched}}$ is the average diameter of etched CNF in nanometer, $\text{Ht}_{\text{unetched}}$ is the average height of unetched CNF in nanometer, $\text{Ht}_{\text{etched}}$ is the average height of etched CNF in nanometer, and x is the temperature in $^{\circ}\text{C}$.

For experiments like those presented earlier, statistical analysis is of pivotal importance. We performed an extensive statistical analysis of the data (details not shown here) and computed 95% confidence intervals. The analysis shows that all the data acquired for a particular temperature fall very close as the range is very short indicating the accuracy of the microscope. The confidence interval data indicate an accuracy of 15 nm for the diameter and within 2 nm for the height for both unetched and etched cases.

CNF dimensional reliability was estimated using the Taguchi approach. Fabrication process does not involve the etching of the CNFs. The etching step in the fabrication procedure was used to etch the SiO_2 layer on the contact pads for the metal exposure. CNFs are well protected inside the SiO_2 layer during this step. A separate etch step was carried out prior to the temperature study in order to etch the CNF dimensions. AFM images of pre- and postetching had shown about 30% variation in the height of the nanofibers. Thus, temperature study was carried out on both the chips.

V. CONCLUSION

Taguchi's approach is successfully applied for the analysis of temperature-dependent changes of VACNFs and the atomic force microscope is effectively implemented as a tool for dimensional measurement and analysis of the CNFs. It can be concluded from this study that the ambient temperature does

have an impact on the fiber dimensions and thus would play a role in their sensing functionality. It is also found that the etchant HF, which is a common etchant in the postfabrication process for etching away the SiO_2 from the Si surface, may not be appropriate as it etches off the VACNF as well. As a result of this finding, we have looked into alternatives such as HCl, H_2SO_4 , and different dilutions of HF. For conclusive reliability information, we plan to directly measure the sensor effectiveness in the future as a function of the parameters.

REFERENCES

- [1] J. Li, *Carbon Nanotubes: Science and Applications*, M. Meyyappan Ed. Boca Raton, FL: CRC Press, 2004.
- [2] M. A. Guillorn, T. E. McKnight, A. Melechko, V. I. Merkulov, P. F. Britt, D. W. Austin, D. H. Lowndes, and M. L. Simpson, "Individually addressable vertically aligned carbon nanofiber based electrochemical probes," *J. Appl. Phys.*, vol. 91, no. 6, pp. 3824–3828, 2002.
- [3] P. He and L. Dai, "Aligned carbon nanotube-DNA electrochemical sensors," *Chem. Commun.*, issue no. 3, pp. 348–349, 2004.
- [4] Y. H. Yun, V. Shanov, M. J. Schulz, Z. Dong, A. Jazieh, W. R. Heineman, H. B. Halsall, D. K. Y. Wong, A. Bange, Y. Tuf, and S. Subramanian, "High sensitivity carbon nanotube tower electrodes," *Sens. Actuators B*, vol. 120, pp. 298–304, 2006.
- [5] P. V. Gerwen, W. Laureyn, W. Laureys, G. Huyberechts, M. O. D. Beeck, K. Baert, J. Suls, W. Sansen, P. Jacobs, L. Hermans, and R. Mertens, "Nanoscaled interdigitated electrode arrays for biochemical sensors," *Sens. Actuators B*, vol. 49, pp. 73–80, 1998.
- [6] J. Li, J. Koehne, A. M. Cassel, H. Chen, Q. Ye, H. T. Ng, J. Han, and M. Meyyappan, "Miniaturized multiplex label-free electronic chip for rapid nucleic acid analysis based on carbon nanotube nanoelectrode arrays," *J. Mater. Chem.*, vol. 14, pp. 676–684, 2004.
- [7] P. U. Arumugam, H. Chen, S. Siddiqui, J. A. P. Weinrich, A. Jejelowo, J. Li, and M. Meyyappan, "Wafer-scale fabrication of patterned carbon nanofiber nanoelectrode arrays: A route for development of multiplexed, ultrasensitive disposable biosensors," *Biosens. Bioelectron.*, vol. 24, pp. 2818–2824, 2009.
- [8] Y. Yun, A. Bange, W. R. Heineman, H. B. Halsall, V. N. Shenov, Z. Dong, S. Pixley, M. Behbani, A. Jazieh, Y. Tu, D. K. Y. Wong, A. Bhattacharya, and M. J. Schulz, "A nanotube array immunosensor for electrochemical detection of antibody-antigen binding," *Sens. Actuators B*, vol. 123, pp. 177–182, 2007.
- [9] Y. Yun, Z. Dong, V. N. Shenov, and M. J. Schulz, "Electrochemical impedance measurement of prostate cancer cells using carbon nanotube array electrodes in a microfluidics channel," *Nanotechnol.*, vol. 18, pp. 465–505, 2007.
- [10] Y. Lin, F. Lu, Y. Tu, and Z. Ren, "Glucose biosensors based on carbon nanotube nanoelectrode ensembles," *Nano Lett.*, vol. 4, no. 2, pp. 191–195, 2004.
- [11] N. Yang, H. Uetsuka, E. Osawa, and C. E. Nebel, "Vertically aligned diamond nanowires for DNA sensing," *Angew. Chem. Int. Ed.*, vol. 47, pp. 5183–5185, 2008.
- [12] F. Patolsky, G. Zheng, and C. M. Lieber, "Fabrication of silicon nanowire devices for ultrasensitive, label-free, real-time detection of biological and chemical species," *Nat. Protocols*, vol. 1, pp. 1711–1724, 2006.
- [13] M. Meyyappan and M. K. Sunkara, *Inorganic Nanowires: Applications, Properties and Characterization*. Boca Raton, FL: CRC Press, 2010, ch. 14.
- [14] C. Li, B. Lei, D. Zhang, X. Liu, S. Han, T. Tang, M. Rouhanizadeh, T. Hsiai, and C. Zhou, "Chemical gating of In_2O_3 nanowires by organic and biomolecules," *Appl. Phys. Lett.*, vol. 83, pp. 4014–4017, 2003.
- [15] J. A. Streifer, H. Kim, B. M. Nichols, and R. J. Hamers, "Covalent functionalization and biomolecular recognition properties of DNA-modified silicon nanowires," *Nanotechnology*, vol. 16, pp. 1868–1873, 2005.
- [16] K. Yang, H. Wang, K. Zon, and X. Zhang, "Gold nanoparticle modified silicon nanowires as biosensors," *Nanotechnology*, vol. 17, pp. S276–S279, 2006.
- [17] R. Rao, C. G. Kumar, R. S. Prakasham, and P. J. Hobbs, "The Taguchi methodology as a statistical tool for biotechnological applications: A critical appraisal," *Biotechnol. J.*, vol. 3, pp. 510–523, 2008.
- [18] G. Guisbiers and L. Buchailot, "Universal size/shape-dependent law for characteristic temperatures," *Phys. Lett. A*, vol. 374, pp. 305–308, 2009.

Uchekukwu C. Wejinya (S'99–M'07) received the B.S. and M.S. degrees in electrical and computer engineering from Michigan State University, East Lansing, in 2000 and 2002, respectively, and the Ph.D. degree in electrical engineering in August 2007 from the same university.

On completing the M.S. degree in 2002, he was with General Motors research and development center where he conducted research on magnetorheological fluid clutch system before returning to graduate school. After completing the Ph.D., he was a Postdoctoral Researcher in the Department of Electrical and Computer Engineering, Michigan State University. In February 2008, he joined the Department of Mechanical Engineering, University of Arkansas, Fayetteville, where he is currently an Assistant Professor. His research interests include mechatronics with emphasis on nanotechnology—nanomaterials for nanosensors including biosensors, chemical; nanoelectronics; control systems design and application, robotics, electronics, microtools for handling and manufacturing of micro- and nanodevices, and modeling and simulation of micro- and nanostructures. He is the author and co-author of more than 50 conference and journal articles, and has presented at several national and international conferences.

Dr. Wejinya served on the administrative committee of IEEE Nanotechnology Council from 2010 to 2012. He has given more than ten invited talks nationally and internationally in his young career. He was among the first group of USA graduate students to participate in the National Science Foundation, East Asia Pacific Summer Institute, Beijing, China, in 2004, where he conducted research at the Chinese Academy of Sciences, Institute of Automation. In 2010, he received the prestigious Chinese Academy of Sciences Fellowship for Young International Scientist Award. He is a member of the American Society of Mechanical Engineers and National Society of Black Engineers.

Siva Naga Sandeep Chalamalasetty (S'10) received the B.Tech degree in biotechnology from Andhra University, Visakhapatnam, India, in 2008. Upon completion of his Bachelors in 2008, he worked as a Mathematics Instructor for 8 months before returning to graduate school. He joined as a Masters student in the Department of Microelectronics and Photonics at the University of Arkansas, Fayetteville, in January 2009. He completed the M.Sc. degree in microelectronics and photonics under the advisement of Dr. Wejinya from the University of Arkansas, in May 2012.

His research interests include microfluidics for drug discovery and drug delivery, Bio-MEMS, micro/nano systems for ultrafast sensing using CNT/Graphene layers and material characterization. He is currently working for Micron Technology Inc., Manassas VA.

Zhuxin Dong (S'07) received the B.E. degree in biomedical engineering from the Shenyang University of Technology, Liaoning, China, in 2005, and the M. Phil. degree in mechanical and automation engineering in the Centre for Micro and Nano Systems (CMNS), Chinese University of Hong Kong, in 2007, where he was a member of 3-D Digital Pen Team. He is currently working toward the Ph.D. degree in the Department of Mechanical Engineering, University of Arkansas, Fayetteville.

His research interest includes calibration and application of MEMS-based μ IMU for human motion sensing and recognition, application of carbon nanotube-based nanodevices, characterization and application of vertically aligned carbon nanofibers, AFM-based indentation and manipulation, and bio-MEMS.

Prabhu U. Arumugam, photograph and biography not available at the time of publication.

Meyya Meyyappan (M'89–SM'96–F'04) received the Ph.D. degree in chemical engineering from Clarkson University, Potsdam, New York, in 1984.

He is the Chief Scientist for Exploration Technology at the Center for Nanotechnology, NASA Ames Research Center, Moffett Field, CA. Until June 2006, he was the Director of the Center for Nanotechnology as well as Senior Scientist. He is a founding member of the Interagency Working Group on Nanotechnology (IWGN) established by the Office of Science and Technology Policy. The IWGN is responsible for putting together the National Nanotechnology Initiative. He has authored or co-authored more than 190 articles in peer-reviewed journals and made more than 200 Invited/Keynote/Plenary Talks in nanotechnology subjects across the world. His research interests include carbon nanotubes and various inorganic nanowires, their growth and characterization, and application development in chemical and biosensors, instrumentation, electronics and optoelectronics.

Dr. Meyyappan is a Fellow of the Electrochemical Society (ECS), AVS, the Materials Research Society (MRS), and the California Council of Science and Technology. In addition, he is a member of the American Society of Mechanical Engineers (ASME) and the American Institute of Chemical Engineers (AIChE). He is currently the IEEE Nanotechnology Council (NTC) Distinguished Lecturer on Nanotechnology, IEEE Electron Devices Society (EDS) Distinguished Lecturer, and was ASME's Distinguished Lecturer on Nanotechnology (2004–2006). He served as the President of the IEEE's Nanotechnology Council during 2006–2007. For his contributions and leadership in nanotechnology, he has received numerous awards including: a Presidential Meritorious Award; NASA's Outstanding Leadership Medal; Arthur Flemming Award given by the Arthur Flemming Foundation and the George Washington University; IEEE Judith Resnick Award; IEEE-USA Harry Diamond Award; AIChE Nanoscale Science and Engineering Forum Award. For his sustained contributions to nanotechnology, he was inducted into the Silicon Valley Engineering Council Hall of Fame in February 2009. For his educational contributions, he has received: Outstanding Recognition Award from the NASA Office of Education; the Engineer of the Year Award (2004) by the San Francisco Section of the American Institute of Aeronautics and Astronautics; IEEE-EDS Education Award; IEEE-EAB (Educational Activities Board) Meritorious Achievement Award in Continuing Education.